BMC Ophthalmology

RESEARCH

Open Access

Comparative analysis of the optic nerve microvasculature between different optic disc phenotypes of normal-tension glaucoma patients

Min Kyung Song[1], Yunhan Lee[2], Joong Won Shin[2], Jin Yeong Lee[2], Ji Wook Hong[2] and Michael S. Kook[2*]

Abstract

Purpose To determine whether the optic nerve head (ONH) and parapapillary choroidal vessel density (VD), measured by optical coherence tomography angiography (OCTA), differ between two common optic disc phenotypes (ODPs) in normal-tension glaucoma (NTG).

Design A retrospective case-control study.

Methods This cross-sectional study analyzed 100 NTG patients with visual field (VF) loss confined to a single hemifield (50 eyes with focal ischemic [FI] ODP and 50 eyes with myopic glaucomatous [MG] ODP, matched for age [≤ 10 years] and VF severity [mean deviation ≤ 1 dB]) as well as 50 healthy eyes. Using OCTA, ONH VD (ONH-VD) was evaluated on a 4.5 × 4.5 mm ONH en-face image using the whole-signal mode. The parapapillary choroidal VD (pCVD) was measured on en-face choroidal layer image within the entire β-parapapillary atrophy (β-PPA) zone using imageJ software. The ONH-VD and pCVD were compared among the three groups. The relationships between ONH-VD and pCVD outcomes and various clinical variables were assessed using linear regression analyses.

Results The average ONH-VD and pCVD were significantly lower in eyes with MG ODPs than those with FI ODPs (56.9% vs. 60.4%, 67.1% vs. 71.8%; both $P < 0.05$). Multivariable linear regression analysis indicated that MG ODP, lower peripapillary retinal nerve fiber layer thickness and VD in the hemiretina, corresponding to hemifield VF loss, in addition to the presence of choroidal microvasculature dropout, were significantly associated with lower ONH-VD and pCVD ($P < 0.05$).

Conclusions The OCTA-measured ONH-VD and pCVD are significantly lower in eyes with MG ODPs rather than FI ODPs. MG ODP is independently associated with lower ONH-VD and pCVD in NTG eyes.

Keywords optic disc phenotype, focal ischemic disc, myopic glaucomatous disc, optical coherence tomography angiography

*Correspondence:
Michael S. Kook
mskook@amc.seoul.kr
[1]Department of Ophthalmology, Ilsan Paik Hospital, Inje University College of Medicine, Goyang, Korea
[2]Department of Ophthalmology, University of Ulsan College of Medicine, Asan Medical Center, 88, Olympic-Ro 43-Gil, Songpa-Gu, Seoul 05505, Korea

Introduction

There are four distinct optic disc appearances or phenotypes (ODPs) recognized in glaucomatous optic nerve heads (ONHs): focal ischemic (FI), myopic glaucomatous (MG), senile sclerotic (SS), and generalized enlargement (GE) [1–3]. The classification of ODPs may be clinically relevant as there are a variety of clinical features associated with them. Glaucoma patients with an FI ODP have a high prevalence of migraines and vasospasms, suggesting that this particular type may be linked to a localized vascular event or optic disc hemorrhage (ODH) [3, 4]. In contrast, an MG ODP can be associated with papillomacular nerve fiber layer damage and central visual field (CVF) defects due to shearing forces across the temporal sides of the lamina cribrosa (LC) [5, 6]. Among the various types of glaucomatous ODPs, FI and MG are the most common phenotypes observed in normal-tension glaucoma (NTG) patients [7].

The recent advent of optical coherence tomography angiography (OCTA) has enabled the clinicians to non-invasively evaluate the microvasculature system of the ONH, peripapillary retina, and macula in glaucoma patients. The superficial peripapillary vessel density (pVD) measured with OCTA has shown good reproducibility in healthy and glaucomatous eyes [8, 9], and also equivalent glaucoma diagnostic capabilities, compared to conventional structural parameters such as the peripapillary retinal nerve fiber layer thickness (pRNFLT) measured by optical coherence tomography (OCT) [10]. Moreover, microvasculature dropout in the parapapillary choroid detected by OCTA has been found to be associated with more advanced glaucomatous visual field (VF) loss as well as reduced pRNFLT, pVD, and parapapillary choroidal thickness in open-angle glaucoma (OAG) eyes [11–13]. As parapapillary choroidal circulation is closely linked to ONH perfusion [11], the assessment of ONH and parapapillary choroid using OCTA may offer an excellent opportunity to study the vascular pathogenesis of OAG.

While an FI ODP is structurally associated with localized neuroretinal rim loss that may be related to a local weakness in the LC or localized vascular event such as ODH [2, 3], an MG ODP results from posterior stretching of the ONH and parapapillary choroid from a myopic axial elongation [11, 14–16]. We hypothesized from this that glaucomatous eyes with different ODPs may exhibit a varying distribution of the vessel density (VD) in the ONH and parapapillary choroid. The aim of our current study was to quantitatively compare the ONH VD (ONH-VD) as well as parapapillary choroidal VD (pCVD) between NTG eyes with FI and MG ODPs, matched for age and glaucoma severity using OCTA. In addition, clinical factors associated with ONH-VD and pCVD were investigated.

Methods

Patients

We performed a retrospective cross-sectional chart review of patients who visited the glaucoma clinic of Asan Medical Center, Seoul, Korea, between November 2021 and June 2022. The Institutional Review Board (IRB) of Asan Medical Center approved the study protocols, and all procedures followed the principles of Declaration of Helsinki. The requirement for informed consent from the subjects was waived by the IRB due to the retrospective nature of the study design.

All subjects had to complete the following initial ophthalmic evaluations: best-corrected visual acuity (BCVA), slit-lamp biomicroscopy, intraocular pressure (IOP) readings with Goldmann applanation tonometry, gonioscopy, axial length (AL), and central corneal thickness (CCT). Other tests included Humphrey field analyzer Swedish Interactive Threshold Algorithm (SITA)-Standard 24 – 2 VF testing (Carl Zeiss Meditec) and dilated color fundus photography, ONH stereoscopic photography, and red-free retinal nerve fiber layer (RNFL) photography. Systolic and diastolic blood pressures (BPs) were measured during outpatient visits, in which the mean arterial pressure (MAP) was estimated as diastolic BP + 1/3 x (systolic BP–diastolic BP), and the mean ocular perfusion pressure (MOPP) as the difference between 2/3 of the MAP and IOP measured during the same visit [17].

Study subjects consisted of NTG patients as well as normal healthy subjects. Inclusion criteria were an age ≥ 18 years, a BCVA of 20/30 or better, refraction between + 3 and − 8 diopters (D) sphere and ± 3D cylinder, open angles revealed by gonioscopy, and visible β-parapapillary atrophy (β-PPA) on fundus photography. NTG patients were required to have (1) glaucomatous VF defects confined to a single hemifield with a mean deviation (MD) of > -10 dB to evaluate eyes with early-to-moderate stage glaucoma [18, 19]; and (2) glaucomatous-appearing ONHs consistent with VF defects without a history of untreated maximum IOP ≥ 22 mmHg during multiple outpatient visits. Glaucomatous VF defects confined to a single hemifield were defined as those with (1) three or more adjacent points with $P < 0.05$ on a pattern deviation (PD) probability map, or with two or more test points with $P < 0.02$ or smaller on a PD probability map in a single hemifield; (2) no clusters of three points with $P < 0.05$ or two points with $P < 0.02$ on both the total deviation and PD probability maps in the opposite hemifield; and (3) a glaucoma hemifield test (GHT) result outside normal limits [18].

All NTG patients that met the initial study inclusion criteria were evaluated consecutively to determine their ODPs with stereoscopic optic disc photographs using a simultaneous stereoscopic viewer (Asahi Pentax Stero Viewer; Tokyo, Japan). Two experienced glaucoma

specialists (M.K.S. and J.W.S), who were blind to the patients' clinical information, independently classified ODPs into one of the following categories, in accordance with Nicolela and Drance's classification method (Fig. 1); (1) FI with localized neuroretinal rim loss at the superior pole, inferior pole, or both, but good preservation of the remaining neuroretinal rim, (2) MG with tilted optic discs showing a temporal crescent with additional glaucomatous damage characterized by neuroretinal rim thinning superiorly, inferiorly, temporally, or a combination thereof in the absence of degenerative myopia, (3) SS with a saucerized and shallow cup exhibiting a relatively pale, moth-eaten neuroretinal rim, parapapillary atrophy, and choroidal sclerosis, or (4) GE with enlarged round cups but no localized neuroretinal rim loss or pallor, and well preserved parapapillary retina. Optic discs with mixed ODP appearances or obscure ODPs in which the observers could not reach a consensus were excluded from the analysis.

In the current study, FI and MG ODPs were selected in the final analysis, since they are the most predominant phenotypes found in Korean NTG patients [7]. MG ODP eyes were consecutively matched in a 1:1 ratio with FI ODP eyes with respect to age (≤ 10 years) and glaucoma severity (mean deviation [MD] ± 1dB) from the enrolled NTG database, as these parameters may affect the ONH-VD and pCVD measurements [10–13]. The healthy eyes were matched to NTG phenotypes by age (≤ 10 years). The healthy controls had bilateral (1) IOP < 21 mmHg in outpatient clinic; (2) no family history of glaucoma; (3) visible β-PPA on fundus photography; (4) normal anterior and posterior segments upon ophthalmologic examination; (5) normal VF test results (defined as a pattern standard deviation within 95% confidence intervals and a GHT result within normal limits); and (6) a non-glaucomatous optic nerve.

Subjects were excluded from the analyses if they displayed cataracts of more than C2, N2, or P2 based on the Lens Opacities Classification System III [20]; severe myopic disc or fundus changes, including posterior staphyloma, that impaired adequate ONH/VF assessment for glaucoma. Other exclusion criteria included unclear ONH boundaries and β-PPA margins; a history of any intraocular surgery or laser procedure; or a history of other ophthalmic or neurologic diseases that could affect VF testing or ONH/retinal evaluations, including age-related macular degeneration, diabetic retinopathy, and retinal vascular occlusive diseases. Eyes with unreliable VF results (fixation loss > 20%, false-positive error > 15%, and false-negative error > 15%) were also excluded.

Peripapillary Vessel Density and Retinal Nerve Fiber Layer Measurements

All subjects underwent OCTA (AngioVue; Optovue, Inc.) during the initial outpatient visit, using an existing and well-described methodology [21]. In the current study, all OCTA images were analyzed using AngioVue software version 2018.1.0.37. The pVD was measured on a

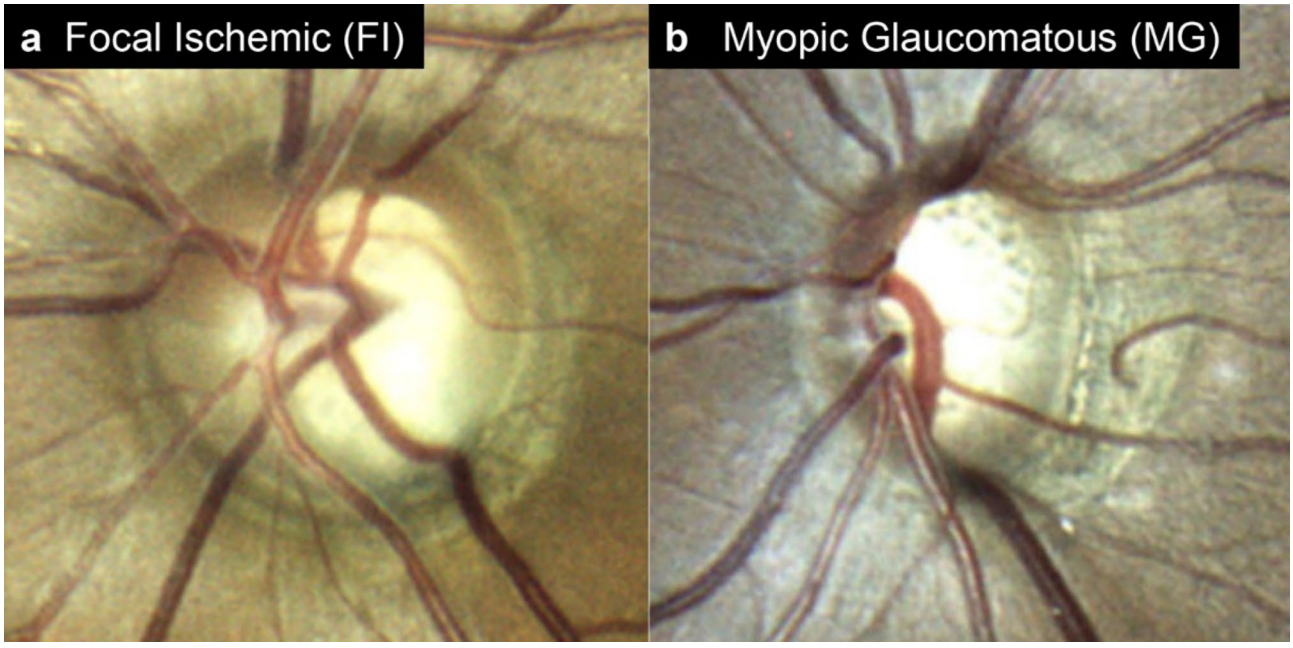

Fig. 1 Two types of glaucomatous optic disc classified in accordance with the procedure of Nicolela and Drance. (**a**) Focal ischemic disc: optic disc had a focal loss of nerve fibers within the neuroretinal rim at the superior pole, inferior pole, or both, but good preservation of the remaining neuroretinal rim. (**b**) Myopic glaucomatous disc: temporal parapapillary atrophy was evident with temporal cupping and neuroretinal rim thinning superiorly, inferiorly, temporally, or a combination thereof in the absence of degenerative myopia

4.5 × 4.5 mm volumetric scan (Angio Disc mode), centered on the ONH. The average pVD was automatically calculated within the RNFL after removal of large vessels within a region defined as a 1000-um-wide elliptical annulus extending from the optic disc boundary. The device provides two 180 degree regional measurements of the pVD (superior, inferior), which represent the superior and inferior hemiretinal values for this parameter. Poor-quality images, defined as those with (1) a signal quality (SQ) score below 7; (2) poor image clarity; (3) motion artifact visualized as an irregular vessel pattern or disc boundary on en-face images; (4) local weak signal due to media opacity (e.g., floaters); or (5) RNFL segmentation errors, were excluded.

The pRNFLT was measured using the Cirrus SD-OCT device in all subjects. The optic disc cube scan calculates this parameter along a circle of 3.45 mm in diameter centered on the ONH. The pRNFLT was measured globally and on each sector of a four-quadrant map. Superior and inferior quadrant measurements of the pRNFLT were used in our analysis to represent its corresponding regional values at the superior and inferior hemiretinae. Poor-quality OCT images defined as those with (1) motion artifacts; (2) poor centration; (3) localized weak signals caused by artifacts such as floaters; (4) segmentation failure; or (5) signal strength < 7, were excluded. In the current study, the pVD/pRNFLT values measured in the hemiretinae of NTG eyes, corresponding to the hemifields with VF loss, were defined as perimetrically-affected hemi-pVD/pRNFLT. Conversely, the values measured in perimetrically-intact hemiretinae were defined as perimetrically-unaffected hemi-pVD/pRNFLT.

ONH-VD and pCVD Measurement using OCTA

In our present analyses, the OCTA whole-signal mode imagery was utilized to measure the ONH-VD on the ONH en-face image. These whole-signal mode images were constructed from all OCTA signals below the internal limiting membrane (ILM) of the ONH. Briefly, the ONH boundary was defined manually as the inner margin of the peripapillary scleral ring identified on scanning laser ophthalmoscopy (SLO) images (Fig. 2a & b, left, red line) [22, 23]. This boundary was applied to the same position of the ONH on the ONH en-face images of OCTA, (Fig. 2c & d, middle, red line) in which the centroid of the ONH was determined using ImageJ software (version 1.52; Wayne Rasband, National Institutes of Health, Bethesda, MD) [22, 23]. The temporal side of the vertical line passing through the ONH centroid with the longest diameter was used in the current analysis (Fig. 2c & d, middle, aqua blue line), since the imaging of deep layers of the ONH using OCT is limited at the nasal side of the optic disc due to large vessels and a thick neural rim [22, 23]. The horizontal line perpendicular to the vertical line was drawn from the centroid of the ONH, which was used to represent the superior and inferior hemi-sector of the ONH (Fig. 2c & d, middle, aqua blue line). For the measurement of ONH-VD, the region of interest (ROI) was marked manually within the temporal ONH, excluding large vessels within the temporal side of the ONH (Fig. 2c & d, middle, aqua blue line) [23]. The superior and inferior hemi-sector ONH-VDs that were measured represented the regional ONH-VD values (i.e., superior vs. inferior). The superior or inferior hemi-sector ONH-VD corresponding to the hemifield with VF loss was defined as the perimetrically-affected hemi-ONH-VD, while that corresponding to the hemifield without VF loss was defined as the perimetrically-unaffected hemi-ONH-VD.

The pCVD was investigated on the 4.5 × 4.5 mm ONH choroidal layer en-face projection image produced by layer segmentation of signals from the retinal pigment epithelium to the inner border of the sclera [11, 13, 19]. For pCVD measurements, the entire β-PPA area was marked as a ROI, while excluding large projecting vessels wider than 3 pixels (approximately ≥ 33 μm) from the retinal layer within the β-PPA on SLO images [13, 19, 24, 25]. This ROI was applied to the same position within the β-PPA of the choroidal en-face image (Fig. 2c & d, middle, yellow line) using ImageJ software. In this current study, the pCVD was analyzed within the entire β-PPA zone, since there is no standard method to regionalize the β-PPA zone into superior and inferior halves to topographically match the location of parapapillary choroidal circulation corresponding to the area of the hemifield, with or without VF loss.

An 8-bit binary slab was created based on the mean threshold algorithm of the ImageJ software using ONH and choroidal layer en-face images [13, 19]. These threshold values are created automatically based on the average of the local grayscale distribution. The selected ROIs for the ONH-VD and pCVD measurement were applied to the 8-bit binary slab of the en-face images. After assigning white pixels to vessels and black pixels to the background, VDs were automatically calculated using ImageJ software as a percentage of vessel pixels within the ONH and β-PPA area relative to the total number of pixels within the ROI [13, 19].

Choroidal Microvasculature Dropout (CMvD) Assessment

The CMvD was defined in this present study as an area of focal complete loss of the choriocapillaries and choroidal microvasculature within the β-PPA on the 4.5 × 4.5 mm ONH choroidal layer en-face projection image, and identified when the minimum angular width of the microvasculature dropout was greater than 200 μm or than the width of the central retinal vein (Fig. 3, red line) [11, 13, 19]. The presence of CMvD was independently assessed

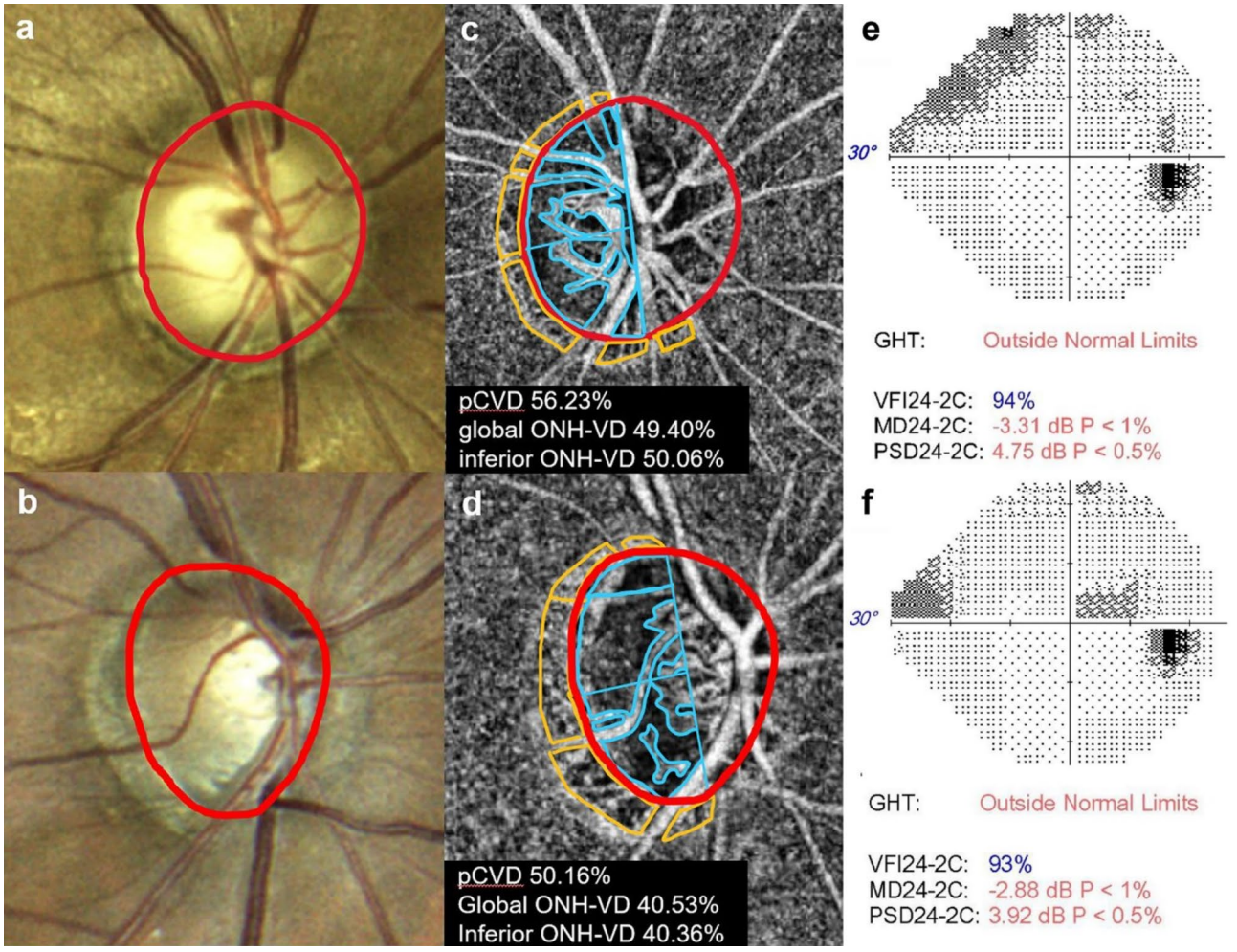

Fig. 2 Representative eyes with a focal ischemic (**a, c, e**) and myopic glaucomatous (**b, d, f**) optic disc phenotype (ODP) of a similar glaucoma severity. (**a**) A 55-year-old male with normal-tension glaucoma (NTG) showing focal ischemic ODP in the right eye. (**b**) A 49-year-old male with NTG in the right eye displaying a myopic glaucomatous ODP. These patients were matched by age and visual field severity (**e, f**). The myopic glaucomatous eye showed lower vessel density within the optic nerve head (ONH) in both the global and perimetrically-affected hemifield (inferior hemiretina) and the entire β-PPA zone than the focal ischemic eye (**c**, **d**)

by M.K.S. and J.W.S, with any discrepancies resolved by a third specialist (M.S.K.).

VF Defect Location

Since ONH-VD and pCVD may be influenced by the location of VF defect—specifically whether the defect is in the central or peripheral VF region—the central and peripheral VF regions were defined according to a previously described method [13]. In brief, a CVF defect at initial presentation was characterized as a glaucomatous VF defect in one hemifield within 10° of fixation, with at least one point at $P < 0.01$ located at the two innermost paracentral points on the pattern deviation plot [13], regardless of any extension into the 10° to 24° VF area. Eyes with peripheral VF defects were defined as those with defect clusters confined solely to the 10° to 24° region within the affected hemifield.

Statistical Analyses

Inter-examiner agreements for determining ODP and the presence of CMvD were assessed using Kappa statistics. A normal distribution was tested using the Kolmogorov–Smirnov test. For comparisons among the groups, one-way analysis of variance (ANOVA) test was performed for continuous variables, based on the normality test. Post hoc analysis was carried out via Tukey's HSD for equal variances and using the Dunnett T3 test for unequal variances. Categorical variables were compared using the chi-square test with the Bonferroni correction for multiple comparisons. To determine the factors associated with global ONH-VD and pCVD, univariable and multivariable linear regression models were built using patient demographics, OCT parameters (i.e., pRNFLT), and the pVD derived from OCTA as independent variables and global ONH-VD and pCVD as the dependent

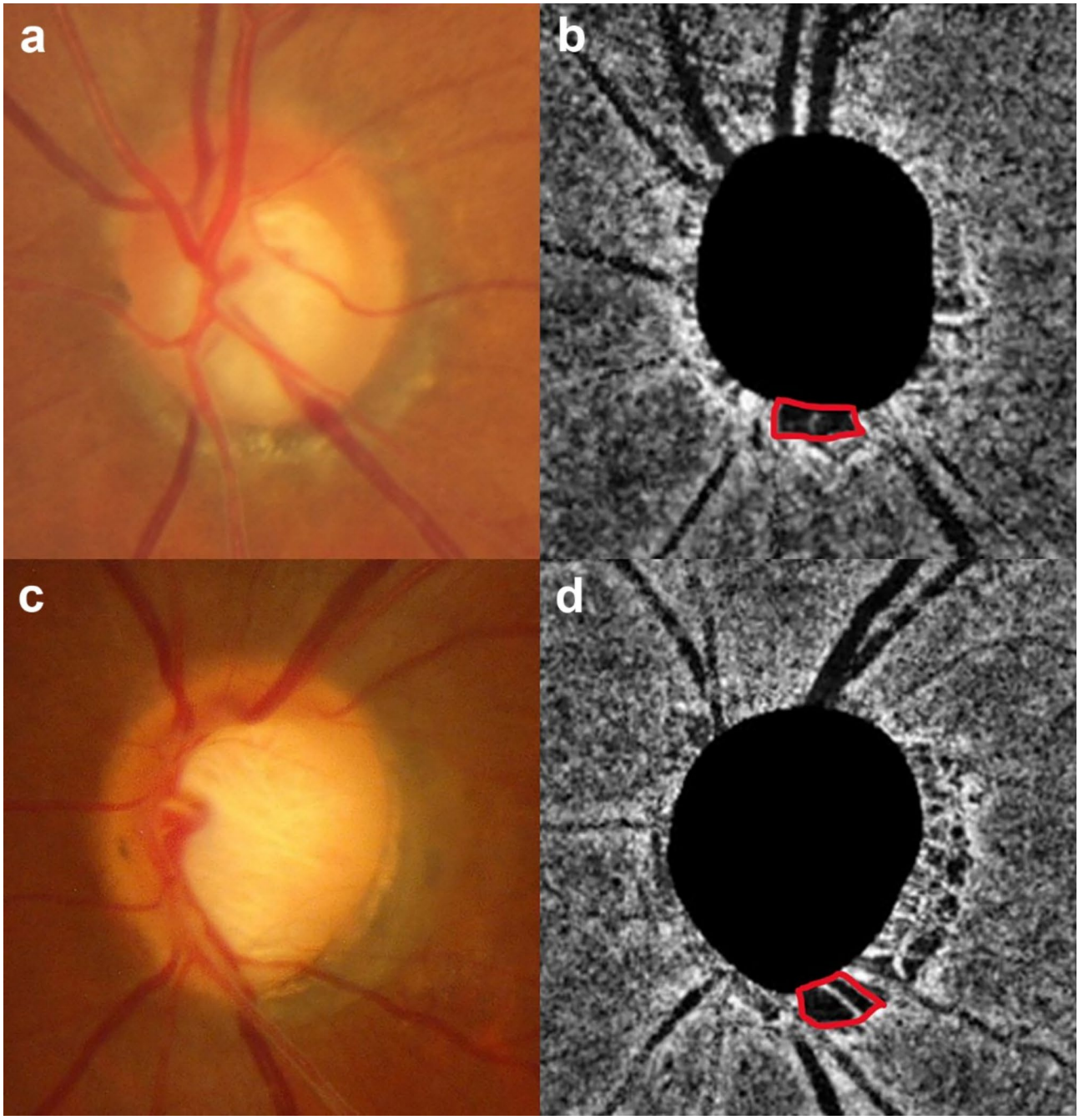

Fig. 3 Representative eyes with focal ischemic (**a, c**) and myopic glaucomatous (**b, d**) optic disc phenotypes (ODPs). (**a**) A 69-year-old female with normal-tension glaucoma (NTG) showing focal ischemic ODP and choroidal microvasculature dropout (CMvD) along the inferior disc border within the β-PPA zone of the left eye (**c**). (**b**) A 60-year-old female with NTG in the left eye displaying myopic glaucomatous ODP and showing CMvD along the inferotemporal disc border within the β-PPA zone of the left eye (**d**). The CMvDs are marked as red lines (**c, d**)

variables. Variables with a P value less than 0.1 in the univariable analyses were included as independent variables in the multivariable model using a backward elimination approach. To avoid multicollinearity within the OCT and OCTA parameters, two separate multivariable models were constructed for global and regional pRNFLT and pVD parameters (i.e., model 1: global; model 2: regional) as independent variables. All statistical analyses were conducted using Statistical Package for Social Science version 22.0 (SPSS, IBM Corp., Armonk, NY), with two-tailed P-values < 0.05 considered statistically significant.

Results

Of the 130 NTG patients and 55 healthy subjects that initially met the eligibility criteria, and were 1:1 matched for this study, 12 (6.4%) and 23 (12.4%) eyes were excluded (i.e., 30 NTG eyes and 5 healthy subjects) due to poor OCTA image clarity and weak signal quality (SQ < 7), respectively, as this would have prevented proper CMvD evaluation or ONH-VD/pCVD quantification. Hence, our final analysis included 50 OAG eyes each in the FI and MG ODP group, matched for age (≤ 10 years) and VF MD (≤ 1 dB). Fifty healthy eyes were also matched to the NTG group for comparison. Inter-examiner agreements regarding the determination of the ODP (k = 0.933; $P < 0.001$) and presence of CMvD were excellent (k = 0.915; $P < 0.001$).

Comparisons of the demographic and clinical characteristics among the three groups are presented in Table 1. There were no significant among-group differences in age, sex, SBP, DBP, MOPP, CCT, baseline IOP, or SQ score. The AL was significantly longer, and SE was more myopic in the MG ODP group compared to either the healthy or FI ODP groups (both $P < 0.001$). The VF MD was similar between the MG and FI ODP group (-5.18 vs. -5.13 dB, $P = 1.00$), while it was significantly lower in both NTG groups compared to the healthy group (both $P < 0.01$). There were no significant differences in the average pRNFLT and pVD between the FI and MG ODP groups when analyzed globally and regionally (i.e., perimetrically-affected and -unaffected hemiretinal regions; all $P > 0.05$). Moreover, there were no significant between group differences in baseline location of hemifield VF defects (i.e., superior vs. inferior) and the location of VF defect in the affected hemified VF loss (central vs. peripheral; both $P > 0.05$).

It was notable however that the global ONH-VD was significantly lower in the MG ODP group than in the FI ODP or healthy groups ($P = 0.02$ for MG vs. FI ODP group and $P < 0.001$ for MG vs. normal controls, respectively). Regionally, the ONH-VDs in both perimetrically-affected and -unaffected hemiretinae were significantly lower in the MG ODP group than in the FI ODP or healthy group ($P < 0.05$ for all comparisons). Moreover, the pCVD was significantly lower in the MG ODP group than in the FI ODP group or control group (74.3 vs. 71.8 vs. 67.1%, post hoc all $P < 0.01$). The prevalence of superior hemifields, as perimetrically–affected hemifields, was similar between the two ODP groups (MG vs. FI; 82% vs. 86%, $P = 0.763$). In each ODP group, the same number of eyes [22 of 50 eyes (44%)] showed the presence of CMvD, showing that the proportion of CMvD occurrence was similar between the FI and MG ODP groups ($P = 1.00$).

The results of the univariable and multivariable linear regression analyses for determining the clinical factors associated with ONH-VD are provided in Table 2. By univariable analyses, MG ODP (β = -5.152, $P < 0.001$), VF MD (β = 0.488, $P = 0.001$), global pRNFLT (β = 0.114, $P = 0.010$), global pVD (β = 0.358, $P < 0.001$), perimetrically-affected hemiretinal pRNFLT (β = 0.061, $P = 0.004$), both perimetrically-affected and -unaffected hemiretinal pVDs (β = 0.356, $P < 0.001$; β = 0.273, $P = 0.001$, respectively), and the presence of CMvD (β = -3.750, $P = 0.002$) were significantly associated with ONH-VD. In two separate multivariable analyses to avoid collinearity of global and regional pRNFLT and pVD, MG ODP (β = -2.858, $P = 0.016$) showed significant associations with ONH-VD in model 1 for global parameter analysis. In regional parameter analysis (model 2), MG ODP (β = -3.315, $P = 0.005$), perimetrically-affected hemiretinal pRNFLT (β = 0.081, $P = 0.022$), and perimetrically-affected hemiretinal pVD (β = 0.469, $P = 0.001$) showed significant associations with ONH-VD.

The results of univariable and multivariable linear regression analyses of the clinical factors associated with pCVD are presented in Table 3. Based on univariate analyses, this parameter showed significant correlations with MG ODP (β = -7.206, P = < 0.001), AL (β = -1.435, $P = 0.001$), and the presence of CMvD (β = -5.558, $P = < 0.001$). In addition, pCVD was found to be significantly associated with VF MD (β = 0.593, $P < 0.001$), average and perimetrically-affected hemiretinal pRNFLT (β = 0.178, $P < 0.001$; β = 0.107, $P < 0.001$, respectively), and average and perimetrically-affected and–unaffected hemiretinal pVD (β = 0.457, $P < 0.001$; β = 0.294, $P < 0.001$; β = 0.192, $P = 0.013$, respectively). Multivariable linear regression analyses which were performed separately for global (model 1) and regional (model 2) parameter analysis, indicated that MG ODP (β = -2.464, $P = 0.042$), AL (β = -0.905, $P = 0.024$), global pVD (β = -2.464, $P = 0.04$) and the presence of CMvD (β= -3.992, $P < 0.001$) remained significantly associated with pCVD in model 1. The analyses for model 2 produced these same correlations with the addition of perimetrically-affected hemiretinal pRNFLT (β = 0.076, $P = 0.001$) and perimetrically-affected hemiretinal pVD (β = 0.221, $P = 0.008$) also having significant associations with pCVD.

Figure 2 shows representative NTG eyes with FI ODP (a, c, e) and MG ODP (b, d, f). The subjects presented were a 55-year-old man with FI ODP in his right eye (a) and a 49-year-old man with MG ODP in his right eye (b). The MG ODP eye showed lower pCVDs in the parapapillary choroid (50.2% vs. 56.2%) and global ONH-VD (40.5% vs. 49.4%) compared to those of the FI ODP eye on OCTA en-face images (c, d). The clinical and demographic characteristics, including age (≤ 10 years) and VF severity (MD ≤ 1dB), were similar between these two eyes (e, f).

Table 1 Demographics and clinical characteristics of the study subjects

	A: Healthy group (*n* = 50)	B: Focal ischemic group (*n* = 50)	C: Myopic glaucomatous group (*n* = 50)	*P* value (A vs. B, A vs. C, B vs. C)
Age (year)	56.2 ± 9.8	58.5 ± 9.8	55.2 ± 9.3	0.229
Sex (M/F)	23/27	25/25	22/28	0.829†
SBP (mmHg)	122.7 ± 16.4	125.9 ± 14.3	121.7 ± 14.5	0.466
DBP (mmHg)	73.7 ± 11.1	76.6 ± 8.3	74.8 ± 8.2	0.422
MOPP (mmHg)	49.3 ± 7.6	52.4 ± 6.2	49.5 ± 6.5	0.113
AL (mm)	24.6 ± 1.3	24.4 ± 1.3	25.7 ± 1.0	**< 0.001** (0.443, **< 0.001**, **< 0.001**)
SE (diopter)	-1.9 ± 2.7	-1.0 ± 2.3	-3.9 ± 3.0	**< 0.001** (0.190, **0.001**, **< 0.001**)
CCT (μm)	542.1 ± 29.1	533.3 ± 28.2	532.5 ± 43.3	0.654
IOP at baseline (mmHg)	15.2 ± 3.2	14.6 ± 2.6	15.6 ± 4.3	0.402
VF MD (dB)	0.47 ± 0.9	-5.18 ± 3.1	-5.13 ± 2.8	**< 0.001** (**< 0.001**, **< 0.001**, 1.000)*
Signal quality score (OCTA)	8.7 (8.4 8.9)	8.4 (8.2 8.6)	8.3 (8.1 8.5)	0.145
Global pRNFLT (μm)	90.3 ± 9.0	72.9 ± 10.2	72.7 ± 8.5	**< 0.001** (**< 0.001**, **< 0.001**, 0.297)
Affected hemi-pRNFLT (μm)	116.0 ± 18.0	72.8 ± 14.4	69.8 ± 11.0	**< 0.001*** (**< 0.001**, **< 0.001**, 0.559)
Unaffected hemi-pRNFLT (μm)	108.0 ± 17.8	100.0 ± 19.8	96.7 ± 17.2	**< 0.001** (0.081, **0.007**, 0.639)
Global pVD (%)	50.46 ± 3.6	44.44 ± 5.0	42.62 ± 5.1	**< 0.001** (**< 0.001**, **< 0.001**, 0.131)
Affected hemi-pVD (%)	49.49 ± 8.1	41.16 ± 5.8	39.94 ± 6.1	**< 0.001** (**< 0.001**, **< 0.001**, 0.642)
Unaffected hemi-pVD (%)	49.42 ± 8.2	47.56 ± 5.4	45.76 ± 5.7	**< 0.001** (0.338, **0.017**, 0.359)
Global ONH-VD (%)	62.05 ± 6.7	60.38 ± 6.2	56.90 ± 6.3	**< 0.001** (0.396, **< 0.001**, **0.020**)
Affected hemi-ONH-VD (%)	62.79 ± 7.4	59.15 ± 7.7	53.81 ± 9.1	**0.001** (**0.048**, **0.001**, **0.032**)
Unaffected hemi-ONH-VD (%)	62.04 ± 6.8	61.94 ± 6.6	57.62 ± 8.4	**0.003** (0.997, **0.008**, **0.010**)
pCVD (%)	74.3 ± 4.4	71.8 ± 5.1	67.1 ± 7.0	**< 0.001** (**0.031**, **< 0.001**, **0.001**)*
Location of (S/I) hemifield loss (%)		44/6 (88%)	41/9 (82%)	0.763
Location of (central/peripheral) hemifield loss (%)		32/18 (64%)	43/7(86%)	0.12
CMvD presence		22/50 (44%)	22/50 (44%)	1.000†

One-way ANOVA test, Tukey HSD as post hoc analysis, * Dunnett T3 test as post hoc analysis

†Chi-square test

Significant P values are shown in bold type

M = male; F = female; SBP = systolic blood pressure; DBP = diastolic blood pressure; MOPP = mean ocular perfusion pressure; AL = axial length; SE = spherical equivalent; CCT = central corneal thickness; IOP = intraocular pressure; VF MD = visual field mean deviation; pRNFLT = peripapillary retinal nerve fiber layer thickness; OCTA = optical coherence tomography angiography; pVD = peripapillary vessel density; pCVD = parapapillary choroidal vessel density; ONH-VD = optic nerve head vessel density; CMvD = choroidal microvasculature dropout; Affected hemi- = perimetrically-affected hemiretinal; Unaffected hemi- = perimetrically-unaffected hemiretinal; S = superior; I = inferior

Discussion

We have here used OCTA to compare ONH-VD and pCVD of FI and MG ODPs in NTG patients, matched for age and glaucoma severity. We found that eyes with MG ODPs had a significantly lower ONH-VD both globally as well as regionally in the perimetrically-affected and -unaffected hemiretinal sectors compared to FI ODP cases, despite both groups having a similar age and glaucoma severity. Moreover, the pCVD was significantly lower in the MG ODP subjects. These findings were further supported by multivariable analyses, indicating that MG ODP is an independent risk factor for lower ONH-VD and pCVD, even after adjusting for confounding factors. Our study findings have thus suggested that ONH-VD and pCVD are inherently affected by ODP in NTG patients, which should be taken into consideration

Table 2 Univariable and multivariable linear regression analyses for factors associated with global optic nerve head vessel density (ONH-VD) in all subjects

	Global optic nerve head vessel density							
	Univariable analysis		**Multivariable analysis 1 (global) ***			**Multivariable analysis 2 (regional) ***		
	β-coefficient	***P* value**	**β-coefficient**	**95% CI**	***P* value**	**β-coefficient**	**95% CI**	***P* value**
Age (year)	-0.018	0.747						
Gender (M to F)	-1.165	0.291						
ODP (MG to FI)	-5.152	**< 0.001**	-2.858	-5.185 to -0.532	**0.016**	-3.315	-5.626 to -1.004	**0.005**
AL (mm)	-0.276	0.542						
CCT (μm)	-0.008	0.627						
Base IOP (mmHg)	-0.178	0.259						
VF MD (dB)	0.488	**0.001**						
Global pRNFLT	0.114	**0.010**						
Affected hemi-pRNFLT	0.061	**0.004**				0.081	0.149 to 0.012	**0.022**
Unaffected hemi-pRNFLT	0.054	0.061						
Global pVD	0.358	**< 0.001**						
Affected hemi-pVD	0.3556	**< 0.001**				0.469	0.191 to 0.746	**0.001**
Unaffected hemi-pVD	0.273	**0.001**						
pCVD (%)	0.120	0.165						
CMvD presence	-3.750	**0.002**	-2.332	-4.758 to 0.093	0.059			

*Multivariable linear regression analyses were performed in separate models for global (model 1) and regional (model 2, hemiretinal) parameters

Significant P values are shown in bold type

M = male; F = female; ODP = optic disc phenotype; MG = myopic glaucomatous; FI = focal ischemic; AL = axial length; CCT = central corneal thickness; IOP = intraocular pressure; VF MD = visual field mean deviation; pRNFLT = peripapillary retinal nerve fiber layer thickness; pVD = peripapillary vessel density; pCVD = parapapillary choroidal vessel density; CMvD = choroidal microvasculature dropout; Affected hemi- = perimetrically-affected hemiretinal; Unaffected hemi- = perimetrically-unaffected hemiretinal

Table 3 Univariable and multivariable linear regression analyses for factors associated with parapapillary choroidal vessel density (pCVD) in all subjects

	Global parapapillary choroidal vessel density							
	Univariable analysis		**Multivariable analysis 1 (global)***			**Multivariable analysis 2 (regional)***		
	β-coefficient	***P* value**	**β-coefficient**	**95% CI**	***P* value**	**β-coefficient**	**95% CI**	***P* value**
Age	0.024	0.670						
Gender (M to F)	-0.157	0.886						
ODP (MG to FI)	-7.206	**< 0.001**	-2.464	-4.833 to -0.095	**0.042**	-3.051	-5.602 to 0.5	**0.019**
AL (mm)	-1.435	**0.001**	-0.905	-1.686 to -0.123	**0.024**	-0.860	-1.654 to -0.067	**0.034**
CCT (μm)	-0.004	0.785						
Base IOP (mmHg)	-0.096	0.540						
VF MD (dB)	0.593	**< 0.001**						
Global pRNFLT (μm)	0.178	**< 0.001**						
Affected hemi-pRNFLT (μm)	0.107	**< 0.001**				0.076	0.031 to 0.122	**0.001**
Unaffected hemi-pRNFLT (μm)	0.042	0.125						
Global pVD (%)	0.457	**< 0.001**	0.251	0.062 to 0.439	**0.011**			
Affected hemi-pVD (%)	0.294	**< 0.001**				0.221	0.060 to 0.382	**0.008**
Unaffected hemi-pVD (%)	0.192	**0.013**						
Global ONH VD (%)	0.031	0.671						
Affected hemi-ONH VD (%)	0.014	0.812						
Unaffected hemi-ONH VD (%)	-0.014	0.834						
CMvD presence	-5.558	**< 0.001**	-3.992	-6.2 to -1.785	**< 0.001**	-4.342	-6.75 to -1.935	**0.001**

*Multivariable linear regression analyses were performed separately in 2 models for global (model 1) and regional (model 2, hemiretinal) parameters

Significant P values are shown in bold type

M = male; F = female; AL = axial length; ODP = optic disc phenotype; MG = myopic glaucomatous; FI = focal ischemic; CCT = central corneal thickness; IOP = intraocular pressure; VF MD = visual field mean deviation; pRNFLT = peripapillary retinal nerve fiber layer thickness; pVD = peripapillary vessel density; ONH-VD = optic nerve head vessel density; CMvD = choroidal microvasculature dropout; Affected hemi- = perimetrically-affected hemiretinal; Unaffected hemi- = perimetrically-unaffected hemiretinal

when managing glaucoma patients with different ODPs determined using OCTA.

Li et al. recently demonstrated using OCTA that the microvascular network may be stretched in the posterior pole of highly myopic eyes [26]. Myopia induces the alteration of the retinal microvascular network, leading to narrowing and a decrease of the pVD in both the superficial and deep retinal layer [26]. In line with this finding, Ekici and colleagues reported lower pVD values in OAG eyes with MG ODP compared to healthy subjects after adjusting for confounders [27]. Nonetheless, to the best of our knowledge, microvascular changes in the ONH itself among different ODPs have not been previously characterized due to technical difficulties in imaging the entire ONH. In our present study, we found a greater ONH-VD decrease in eyes with MG ODP based on the OCTA whole-signal mode image, capturing all ONH signals below the ILM.

Myopic optic disc changes encompass a series of morphological alterations due to the stretching of papillary and peripapillary structures during axial elongation [28]. Hence, it could be inferred that these structural changes occur in a global pattern involving the entire ONH in the MG ODP group. This speculation is supported by our present observation that ONH-VDs in both hemi-sectors were significantly lower in eyes with MG ODPs compared to the FI ODP and healthy control groups. In contrast, our FI ODP eyes showed similar ONH-VD in the hemi-sector corresponding to perimetrically-unaffected hemifield when compared to healthy eyes, while the ONH-VD in the hemi-sector corresponding to perimetrically-affected hemifield was significantly lower in the FI ODP group than in the healthy group. This indicated that FI ODP is associated with localized ONH-VD loss corresponding to a single hemifield VF loss.

Our current analyses revealed that the pCVD was lower in the MG ODP subjects compared to the other two groups. Previous studies have reported that myopic eyes have a thinner choroid, including the parapapillary choroid, due to the lower VD and smaller vessel diameter in the choroidal layer [25, 29, 30]. Moreover, choroidal VD has been reported to have a strong negative relationship with AL, since posterior axial elongation induces a smaller vessel diameter with reduced VD in the choroid [31]. Since the MG ODP eyes had a greater AL than those with FI ODP (i.e., 25.7 mm vs. 24.4 mm) in our current study population, AL differences may possibly explain our current findings. As a lower pCVD is a known vascular risk factor for future glaucoma progression [24], the clinical relevance of its association with MG ODP remains to be further determined in future longitudinal studies.

In our present multivariable analyses, MG ODP, lower pRNFLT and pVD in the perimetrically-affected hemiretina, and CMvD were the factors found to be associated with lower ONH-VD and pCVD in NTG patients. These findings suggest that optic disc appearance in NTG eyes (i.e., MG ODP) is an independent factor for low ONH-VD and pCVD, which may perhaps be related to the risk of future disease progression. The association between pRNFLT and pVD in the perimetrically-affected hemiretinae and ONH-VD/pCVD may indicate a close relationship between ONH-VD/pCVD and glaucoma severity. Although the temporal relationship remains to be clarified, a lower ONH-VD/pCVD value, which indicates poor microvascular perfusion around and within the ONH, can lead to a greater degree of glaucomatous damage, resulting in significant positive associations between pRNFLT and pVD in the perimetrically-affected hemiretinae and ONH-VD/pCVD.

The parapapillary choroid is closely linked to ONH perfusion since it is proximal to the ONH and receives its blood supply from the short posterior ciliary arteries [11, 32–34]. Since CMvD represents an area of complete loss of microvasculature within the parapapillary choroid, it is not unexpected to find that its presence was significantly associated with a diminished pCVD, as shown in our multivariable analyses, although the association between CMvD and ONH-VD decrease showed borderline significance only ($P = 0.059$). It could be postulated therefore that the presence of CMvD in association with a lower pCVD and ONH-VD may increase the risk of future glaucoma progression. Indeed, recent studies have demonstrated that VF progression and progressive RNFL thinning are more frequently observed in OAG eyes with CMvD than in those without, despite their having similar IOP profiles during follow-up [25, 35].

From our present multivariable analysis, a longer AL was independently associated with a lower pCVD, which was not a surprising observation. Although the MG ODP eyes in this present study cohort were selected based on the clinical appearance of the optic disc, without taking AL into account, a significant correlation between MG ODP and AL cannot be ruled out (AL: 25.7 mm for MG ODP group). Since myopic eyes have thinner choroid around the ONH, along with lower VD and smaller vessel diameter in the choroidal layer [29, 30], and the choroidal VD has a strong negative relationship with AL [25], our finding of a negative association between AL and pCVD was consistent with those of earlier reports.

Prior studies have shown that average pRNFLT decreases with longer AL and that highly myopic eyes have significantly thicker temporal pRNFLT and thinner pRNFLTs in the non-temporal sectors compared with eyes with low myopia [36, 37]. In the present study, however, the MG ODP eyes had similar pRNFLT globally and regionally compared to the FI ODP group. Moreover, while eyes with high myopia have a decreased pVD

compared with emmetropic eyes [38], there were no significant differences in the pVD values between these two ODP groups in the present study. This discrepancy might be attributable to our strict matching between the two groups in terms of age and glaucoma severity. Since pVD is known to be well-correlated with pRNFLT in glaucomic eyes [10, 11], and both of our ODP study groups had similar pRNFLT after matching for VF severity, no significant difference in pVD was found either between these two groups based on our present analyses.

In a previous cross-sectional study of primary open-angle glaucoma (POAG) and NTG eyes, patients with advanced NTG predominantly displayed MG ODP, with only a small proportion of eyes showing FI ODP [39]. These findings suggest that MG ODP may lead to a faster rate of VF loss and a tendency toward a faster rate of optic disc deterioration than FI ODP, indicating that ODPs might be related to the degree or speed of glaucoma progression. The ONH-VD and pCVD values were significantly lower in our present MG ODP group, suggesting an association with a greater likelihood of disease progression over time i.e., leading to advanced glaucoma. Prospective longitudinal studies are needed to test this proposition.

The clinical relevance of our findings suggests that when utilizing raw ONH-VD and pCVD values from OCTA for glaucoma diagnosis, it is essential to account for variations in ODP among glaucomatous eyes, as these parameters are inherently influenced by ODP in NTG patients. Given that myopia results in significantly lower ONH-VD and pCVD in eyes with MG ODP compared to those with FI ODP—despite both groups having similar age and VF loss—greater emphasis may be placed on functional assessments, such as VF testing, rather than structural measures like ONH-VD or pCVD for diagnosing and monitoring glaucoma in eyes with MG ODP.

There were several limitations to this present study of note. First, a degree of subjectivity might have affected the classification of ODPs or determination of the CMvD presence. However, these decisions were made by consensus between two experienced graders and there was good interobserver agreement ($k = 0.933$ and 0.915; $P < 0.001$, respectively). Another possible limitation was that we included only two ODPs (i.e., FI and MG ODP) in our study as GE and SS ODPs are relatively uncommon in NTG patients [7]. It remains to be assessed whether GE and SS ODPs might have different impacts on ONH-VD and pCVD distribution. There was also an inability to generalize our findings to patients with high-tension glaucoma (classified by an IOP level > 21 mmHg) and to non-Asian individuals, as only Korean NTG patients were included in our current cohorts. Another limitation of our study is that our patient cohort included eyes with early-to-moderate stage glaucoma, characterized by VF defects confined to a single hemifield and an MD greater than −10 dB. As a result, our findings may not be applicable to eyes with advanced glaucoma. Additionally, the cross-sectional design of our study prevented us from examining the temporal relationship between different ODPs and the reduction of ONH-VD and pCVD over time. Furthermore, our study design does not allow us to determine whether lower ONH-VD and pCVD are associated with an increased risk of future glaucoma progression, which should be further investigated through longitudinal studies. We must note also that our ONH-VD measurements were performed manually using the whole-signal mode image of OCTA, which can be subject to various artifacts. To overcome this limitation as much as possible, only well-visualized ONH borders and β-PPA zones were included and analyzed with the previously published methodology [22, 23]. In addition, since there is currently no commercially available software to automatically assess pCVD regionally, we manually evaluated this parameter within the entire the entire β-PPA zone using ImageJ software, which has been previously validated [19, 21, 24, 25]. Finally, it is possible that ocular anti-glaucoma eye drops can affect ocular blood flow in glaucoma patients [40]. Hence, our current findings must be interpreted with consideration of the possible compounding effects of anti-glaucoma eye drops on OCTA measurements, since our NTG patients were receiving this treatment.

In conclusion, our results show that ONH-VD and pCVD are affected by the ODP, even after controlling for other confounding factors. ONH-VD is significantly lower globally, and even in the hemi-sectors corresponding to perimetrically-intact hemifields, in MG ODP compared to FI ODP. The pCVD is also significantly lower in MG ODP eyes. Clinicians must thus be aware of the impact of ODP on the ONH-VD and pCVD when managing NTG patients using OCTA.

Abbreviations

ONH	optic nerve head
VD	vessel density
OCTA	optical coherence tomography angiography
ODPs	optic disc phenotypes
NTG	normal-tension glaucoma
VF	visual field
FI	focal ischemic
MG	myopic glaucomatous
pCVD	parapapillary choroidal VD
β-PPA	β-parapapillary atrophy
SS	senile sclerotic
GE	generalized enlargement
ODH	optic disc hemorrhage
CVF	central visual field
LC	lamina cribrosa
pVD	peripapillary vessel density
pRNFLT	peripapillary retinal nerve fiber layer thickness
OAG	open-angle glaucoma
IRB	Institutional Review Board
BCVA	best-corrected visual acuity

IOP	intraocular pressure
AL	axial length
CCT	central corneal thickness
BPs	blood pressures
MAP	mean arterial pressure
MOPP	mean ocular perfusion pressure
MD	mean eviation
GHT	glaucoma hemifield test
SQ	signal quality
ILM	internal limiting membrane
SLO	scanning laser ophthalmoscopy
ROI	region of interest
CMvD	Choroidal Microvasculature Dropout
POAG	primary open-angle glaucoma

Acknowledgements
None.

Author contributions
Conception and design: M.S.KAcquisition, analysis and interpretation: M.K.S., Y.L., J.W.S., J.Y.L., J.W.H. and M.S.K.Drafting of the manuscript: M.K.S. and M.S.K.Critical revision of the manuscript for important intellectual content: M.K.S., Y.L. and M.S.K.Supervision: M.S.K.

Funding
This research did not receive any specific grant from funding agencies in the public, commercial, or not-for-profit sectors.

Data availability
The datasets used and/or analysed during the current study are available from the corresponding author on reasonable request.

Declarations

Competing interests
The authors declare no competing interests.

Ethics approval and consent to participate
The Institutional Review Board (IRB) of Asan Medical Center approved the study protocols, and all procedures followed the principles of Declaration of Helsinki. The requirement for informed consent from the subjects was waived by the IRB due to the retrospective nature of the study design.

Consent for publication
Not applicable.

Received: 18 October 2024 / Accepted: 17 March 2025
Published online: 26 March 2025

References

1. Nicolela MT, Drance SM. Various glaucomatous optic nerve appearances: clinical correlations. Ophthalmology. 1996;103:640–9.
2. Reis AS, Artes PH, Belliveau AC, Leblanc RP, Shuba LM, Chauhan BC, et al. Rates of change in the visual field and optic disc in patients with distinct patterns of glaucomatous optic disc damage. Ophthalmology. 2012;119:294–303.
3. Nicolela MT, McCormick TA, Drance SM, Ferrier SN, LeBlanc RP, Chauhan BC. Visual field and optic disc progression in patients with different types of optic disc damage: a longitudinal prospective study. Ophthalmology. 2003;110:2178–84.
4. Ekici E, Moghimi S, Hou H, Proudfoot J, Zangwill LM, Do JL, et al. Central visual field defects in patients with distinct glaucomatous optic disc phenotypes. Am J Ophthalmol. 2021;223:229–40.
5. Choi JA, Park HY, Shin HY, Park CK. Optic disc characteristics in patients with glaucoma and combined superior and inferior retinal nerve fiber layer defects. JAMA Ophthalmol. 2014;132:1068–75.
6. Lee KM, Lee EJ, Kim TW. Lamina cribrosa configuration in tilted optic discs with different tilt axes: a new hypothesis regarding optic disc tilt and torsion. Invest Ophthalmol Vis Sci. 2015;56:2958–67.
7. Lee JR, Kim S, Lee JY, Back S, Lee KS, Kook MS. Is myopic optic disc appearance a risk factor for rapid progression in medically treated glaucomatous eyes with confirmed visual field progression? J Glaucoma. 2016;25:330–7.
8. Venugopal JP, Rao HL, Weinreb RN, Pradhan ZS, Dasari S, Riyazuddin M, et al. Repeatability of vessel density measurements of optical coherence tomography angiography in normal and glaucoma eyes. Br J Ophthalmol. 2018;102:352–7.
9. Manalastas PIC, Zangwill LM, Saunders LJ, Mansouri K, Belghith A, Suh MH, et al. Reproducibility of optical coherence tomography angiography macular and optic nerve head vascular density in glaucoma and healthy eyes. J Glaucoma. 2017;26:851–9.
10. Rao HL, Pradhan ZS, Weinreb RN, Reddy HB, Riyazuddin M, Dasari S, et al. Regional comparisons of optical coherence tomography angiography vessel density in primary open-angle glaucoma. Am J Ophthalmol. 2016;171:75–83.
11. Suh MH, Zangwill LM, Manalastas PI, Belghith A, Yarmohammadi A, Medeiros FA, et al. Deep retinal layer microvasculature dropout detected by the optical coherence tomography angiography in glaucoma. Ophthalmology. 2016;123:2509–18.
12. Yarmohammadi A, Zangwill LM, Diniz-Filho A, Suh MH, Yousefi S, Saunders LJ, et al. Relationship between optical coherence tomography angiography vessel density and severity of visual field loss in glaucoma. Ophthalmology. 2016;123:2498–508.
13. Kwon J, Shin JW, Lee J, Kook MS. Choroidal microvasculature dropout is associated with parafoveal visual field defects in glaucoma. Am J Ophthalmol. 2018;188:141–54.
14. Quigley HA. Reappraisal of the mechanisms of glaucomatous optic nerve damage. Eye (Lond). 1987;1(Pt 2):318–22.
15. Cahane M, Bartov E. Axial length and scleral thickness effect on susceptibility to glaucomatous damage: a theoretical model implementing Laplace's law. Ophthalmic Res. 1992;24:280–4.
16. Samra WA, Pournaras C, Riva C, Emarah M. Choroidal hemodynamic in myopic patients with and without primary open-angle glaucoma. Acta Ophthalmol. 2013;91:371–5.
17. Kwon J, Lee J, Choi J, Jeong D, Kook MS. Association between nocturnal blood pressure dips and optic disc hemorrhage in patients with normal-tension glaucoma. Am J Ophthalmol. 2017;176:87–101.
18. Anderson DR. Automated static perimetry. St. Louis: Mosby; 1992.
19. Jo YH, Shin JW, Song MK, Won HJ, Kook MS. Choroidal microvasculature dropout is associated with generalized choroidal vessel loss within the beta-parapapillary atrophy in glaucoma. Am J Ophthalmol. 2020;215:37–48.
20. Chylack LT Jr., Wolfe JK, Singer DM, Leske MC, Bullimore MA, Bailey IL, et al. The lens opacities classification system III. The longitudinal study of cataract study group. Arch Ophthalmol. 1993;111:831–6.
21. Jia Y, Tan O, Tokayer J, Potsaid B, Wang Y, Liu JJ, et al. Split-spectrum amplitude-decorrelation angiography with optical coherence tomography. Opt Express. 2012;20:4710–25.
22. Akagi T, Zangwill LM, Shoji T, Suh MH, Saunders LJ, Yarmohammadi A, et al. Optic disc microvasculature dropout in primary open-angle glaucoma measured with optical coherence tomography angiography. PLoS ONE. 2018;13:e0201729.
23. Song MK, Shin JW, Lee JY, Hong JW, Kook MS. Choroidal microvasculature dropout is spatially associated with optic nerve head microvasculature loss in open-angle glaucoma. Sci Rep. 2021;11:15181.
24. Park HY, Shin DY, Jeon SJ, Park CK. Association between parapapillary choroidal vessel density measured with optical coherence tomography angiography and future visual field progression in patients with glaucoma. JAMA Ophthalmol. 2019;137:681–8.
25. Kwon JM, Weinreb RN, Zangwill LM, Suh MH. Parapapillary deep-layer microvasculature dropout and visual field progression in glaucoma. Am J Ophthalmol. 2019;200:65–75.
26. Li M, Yang Y, Jiang H, Gregori G, Roisman L, Zheng F, et al. Retinal microvascular network and microcirculation assessments in high myopia. Am J Ophthalmol. 2017;174:56–67.
27. Ekici E, Moghimi S, Bowd C, Hou H, Penteado RC, Proudfoot J, et al. Capillary density measured by optical coherence tomography angiography in glaucomatous optic disc phenotypes. Am J Ophthalmol. 2020;219:261–70.
28. Hu R, Wu Q, Yi Z, Chen C. Multimodal imaging of optic nerve head abnormalities in high myopia. Front Neurol. 2024;15:1366593.
29. Kimura Y, Akagi T, Hangai M, Takayama K, Hasegawa T, Suda K, et al. Lamina cribrosa defects and optic disc morphology in primary open angle glaucoma with high myopia. PLoS ONE. 2014;9:e115313.

30. Hasegawa T, Akagi T, Hangai M, Yamada H, Suda K, Kimura Y, et al. Structural dissociation of optic disc margin components with optic disc tilting: a spectral domain optical coherence tomography study. Graefes Arch Clin Exp Ophthalmol. 2016;254:343–9.
31. Nakazawa T, Shimura M, Ryu M, Himori N, Nitta F, Omodaka K, et al. Progression of visual field defects in eyes with different optic disc appearances in patients with normal tension glaucoma. J Glaucoma. 2012;21:426–30.
32. Anderson DR, Braverman S. Reevaluation of the optic disk vasculature. Am J Ophthalmol. 1976;82:165–74.
33. O'Brart DP, de Souza Lima M, Bartsch DU, Freeman W, Weinreb RN. Indocyanine green angiography of the peripapillary region in glaucomatous eyes by confocal scanning laser ophthalmoscopy. Am J Ophthalmol. 1997;123:657–66.
34. Michelson G, Langhans MJ, Groh MJ. Perfusion of the juxtapapillary retina and the neuroretinal rim area in primary open angle glaucoma. J Glaucoma. 1996;5:91–8.
35. Park HL, Kim JW, Park CK. Choroidal microvasculature dropout is associated with progressive retinal nerve fiber layer thinning in glaucoma with disc hemorrhage. Ophthalmology. 2018;125:1003–13.
36. Kang SH, Hong SW, Im SK, Lee SH, Ahn MD. Effect of myopia on the thickness of the retinal nerve fiber layer measured by Cirrus HD optical coherence tomography. Invest Ophthalmol Vis Sci. 2010;51:4075–83.
37. Hwang YH, Yoo C, Kim YY. Myopic optic disc tilt and the characteristics of peripapillary retinal nerve fiber layer thickness measured by spectral-domain optical coherence tomography. J Glaucoma. 2012;21:260–5.
38. Wang X, Kong X, Jiang C, Li M, Yu J, Sun X. Is the peripapillary retinal perfusion related to myopia in healthy eyes? A prospective comparative study. BMJ Open. 2016;6:e010791.
39. Nakazawa T, Fuse N, Omodaka K, Aizawa N, Kuwahara S, Nishida K. Different types of optic disc shape in patients with advanced open-angle glaucoma. Jpn J Ophthalmol. 2010;54:291–5.
40. Feke GT, Bex PJ, Taylor CP, Rhee DJ, Turalba AV, Chen TC, et al. Effect of brimonidine on retinal vascular autoregulation and short-term visual function in normal tension glaucoma. Am J Ophthalmol. 2014;158:105–12. e1.

Publisher's note